Simulation of pore evolution under laser remelting in SLM process

Yanping Miao[1], Zhiwen Li[2], Hui Lei[3]
[1, 2, 3]School of Mechanical Engineering, Jiangxi Technical College of Manufacturing, Nanchang, China
[2]School of Mechanical and Electronic Engineering, Jingdezhen Ceramic University, Jingdezhen, China
[2]Corresponding author
E-mail: [1]*miaoyanping1@jxmtc.edu.cn*, [2]*lizhiwen@jxmtc.edu.cn*, [3]*leihui@jxmtc.edu.cn*

Received 29 January 2026; accepted 18 March 2026; published online 8 June 2026
DOI https://doi.org/10.21595/vp.2026.26059

76th International Conference on Vibroengineering in Tashkent, Uzbekistan, April 28-29, 2026

Abstract. In the process of selective laser melting (SLM) forming, pore defects can seriously affect the quality of formed parts. In this paper, the effectiveness of laser remelting to eliminate the pore defects of SLM formed parts was analyzed experimentally. Based on the level set method, a numerical simulation of multi-physics finite element model was established to analyze the mechanism of pore evolution during laser remelting. It is found that the pore evolution is significantly affected by the Marangoni effect at the micro scale. Affected by the Marangoni effect, during the evolution process, the porosity doesn't rise vertically. Instead, it moves towards the tail area of the molten pool while rising. The essence of pore evolution is fluid mass transfer. Moreover, the effectiveness of laser remelting in eliminating porosity has been verified through experiments.

Keywords: additive manufacturing, SLM, pore evolution, simulation, laser remelting, Marangoni effect.

1. Introduction

Selective laser melting (SLM) is a powder bed additive manufacturing technology that forms solid parts by layer-by-layer melting and solidifying metal powders. It has been widely applied in aerospace, industrial automation, medical engineering and other fields. During SLM forming, factors such as laser power, powder characteristics and scanning speed easily cause pore defects, which seriously affect part performance. As a post-processing or optimization process, laser remelting can enhance inter-layer metallurgical bonding by reducing molten pool width and increasing molten pool overlap rate, while providing overflow time for trapped gas in the molten pool, thus reducing or eliminating pores. In recent studies, Yasa and Kruth [1] optimized 316L stainless steel remelting parameters (scanning speed: 200-400 mm/s, power: 85-95 W) and reduced porosity to 0.032 %. Qiu et al. [2] eliminated lack-of-fusion holes in 316L stainless steel via different powers and scanning strategies. Demir and Previtali [3] found that remelting and preheating of 18Ni300 maraging steel can reduce porosity but may increase dimensional errors.

In summary, laser remelting significantly reduces SLM part porosity. However, experimental analysis of micro-pore evolution is difficult due to metal opacity and rapid dynamic processes, making numerical simulation a key research method. Existing laser remelting simulation studies are limited. This paper constructs a level set-based multi-physical field model, analyzes pore evolution mechanisms, simulates effects of mass transfer, Marangoni effect and energy density, and studies pore evolution laws under different process parameters through numerical simulation.

2. Numerical simulation

2.1. Modeling

Numerical simulation, when compared to experimental methods, provides an intuitive, cost-

effective, and efficient means of investigating the pore evolution mechanism during laser remelting. In this study, COMSOL Multiphysics simulation software was used to build a two-dimensional finite element analysis model. The model was established according the Level-set method and combines the Marangoni effect and mass transfer to simulate the interaction between laser and material, as clearly shown and precisely demonstrated in Fig. 1.

Calculation Domain L×H of the simulation model is 800 μm×350 μm, Domain 1 is a solid 316L alloy plate formed by SLM, Domain 3 are pores with a diameter of 10 μm, filled with argon, its depth is represented by d_{pore}, and the horizontal distance between the pores is represented by l_{pore}. In the simulation model, the horizontal distance between the two adjacent pores is the same, l_{pore} = 50 μm. Domain 2 is a shielding gas (argon) with a height of 150 μm. In addition, to simplify the model calculations, the gasification of the material is disregarded. A continuous Gaussian heat source, represented by a single-channel laser beam, scans the upper surface of the 316L stainless steel, initiating at $X = 0$ and progressing along the X-axis. To enhance the accuracy and efficiency of the simulation, the mesh at the liquid-solid interface was refined locally. Finally, the grid cells in the simulation model amounts to 118,505 in total, alongside 141,073 internal degrees of freedom, encompassing the entire simulation domain. The thermophysical property parameters of the materials utilized in the numerical simulation are detailed in Table 1.

There are multiphase transition and complex physical phenomena in laser remelting process, to streamline the numerical model, several assumptions are made:

(a) Since the calculation step time is much longer than the pulse interval of the laser, the laser is assumed to be a continuous Gaussian heat source [4].

(b) The mass loss due to gasification is minimal and therefore negligible [4].

(c) The laser absorptivity of 316L stainless steel is considered to be constant [5].

(d) Define the fluid in the molten pool as an incompressible Newtonian fluid and make the flow laminar [6].

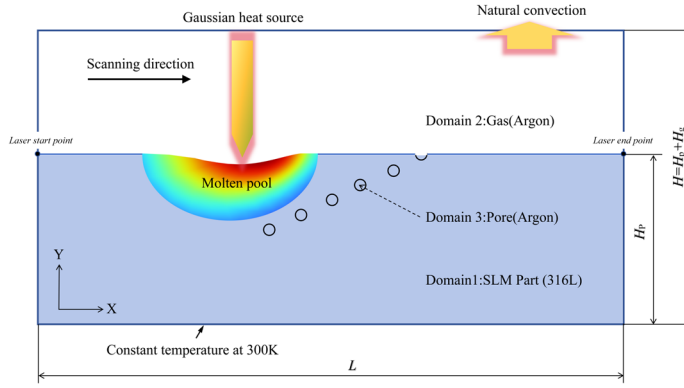

Fig. 1. Numerical simulation model of laser remelting

Table 1. Thermophysical properties of 316L stainless steel

Property (unit)	Nomenclature	Value	Ref.
Liquidus temperature (K)	T_l	1723.0	[1]
Solidus temperature (K)	T_s	1650.0	[1]
Evaporation temperature (K)	T_v	3080.0	[1]
Specific heat (J·Kg^{-1}·K^{-1})	C_s	$4.186 \times 10^3 \times (0.1097 + 3.174 \times 10^{-5}T)$	[1]
Solid density (g/cm^3)	ρ_s	$8.0842 - 4.2086 \times 10^{-4}T - 3.8942 \times 10^{-8}T^2$	[1]
Liquid density (g/cm^3)	ρ_l	$7.4327 + 3.9338 \times 10^{-5}T - 1.8007 \times 10^{-7}T^2$	[1]
Thermal conductivity (W·m^{-1}·K^{-1})	K	$\begin{cases} 9.248 + 1.571 \times 10^{-2}T, & T \le 1723K \\ 12.41 + 3.279 \times 10^{-3}T, & T > 1723K \end{cases}$	[1]
Latent heat of fusion (J·Kg^{-1})	L_m	2.7×10^5	[1]

2.2. Heat source and thermal boundary conditions

The heat source in the laser remelting process is regarded as a continuous Gaussian heat source, and its equation is as follows [7]:

$$Q_{laser} = \frac{2AP_{laser}}{\pi r_0^2} \cdot \exp\left(\frac{-2(x_i - x_0 - v_{laser}t)^2}{r_0^2}\right), \tag{1}$$

where r_0 is radius of the laser beam, Q_{laser} is the energy input of the laser, x_0 is the initial coordinate position of the laser beam, x_i is the center coordinate position of the laser beam, A is absorption coefficient of the laser, v_{laser} is scanning speed of the laser, and p_{laser} is the laser power.

The top section of the model in domain 2 is specifically configured for natural convection. Notably, a convection coefficient of 80W·m^{-2}·K^{-1} is assigned to this setup. The upper emissivity of domain 1 is set to ε, corresponding to the Stefan-Boltzmann law [8].

2.3. Marangoni effect, surface tension and recoil pressure

In order to ensure the feasibility and effectiveness of the numerical simulation, the surface boundary of the simulation model is set to zero displacement. The surface change of the molten pool caused by the Marangoni effect can be expressed by the following equation [9]:

$$\sigma = \kappa\gamma \cdot n_{surface} + \nabla_s\gamma, \tag{2}$$

where σ is the surface tension, $n_{surface}$ is the unit of normal to the local surface, κ is the interface curvature, γ is the surface tension coefficient, $n_{surface}$ is the unit of normal to the local surface, ∇_s is the surface gradient operator.

When the temperature of the molten pool reaches the boiling point and the molten metal vaporizes, the top of the molten pool will recoil under the action of metal steam, and the formula for the recoil pressure is as follows [10]:

$$P_{recoil} = 0.54P_a \cdot \exp\left(1 - \frac{K_b T_{surface}}{\lambda T_b}\right), \tag{3}$$

where P_a stands for the ambient pressure, set as 1 atm, K_b is 8.617×10^5 eV·K^{-1}, stands for the Boltzmann constant, λ is 4.9 eV per atom, stands for the gasification potential heat per atom [11], $T_{surface}$ stands for the surface temperature of the molten pool, T_b is 3080K, stands for the boiling point of 316L stainless steel.

3. Numerical simulation results and discussion

Fig. 2 shows the pore evolution diagram when the laser remelting power is 100 W and the scanning speed is 1 m/s. In order to more intuitively compare the process of pore retention and elimination, P2 pore (marked in Fig. 1) with a depth of 40 μm and P3 pore with a depth of 30 μm are selected for comparison, and the distance between the two pores in the horizontal direction is 50 μm.

As shown in Fig. 2, where the black arrow indicates the velocity direction of the molten fluid, and the magnitude of the fluid velocity is represented by the length of the arrow, and it can be seen from the figure that the velocity increases dramatically when porosity forms new bubbles in the molten pool or when rupture occurs, and under the action of the Marangoni effect, a fluid vortex is formed around the porosity. In the process of pore evolution, at 140 μs, both P2 and P3 holes are at the bottom of the molten pool, and slight deformation occurs under the action of the

molten pool fluid. With the evolution of the molten pool, at 165 μs, the P3 hole had risen to the middle of the molten pool and was divided into two small bubbles under the action of the molten pool fluid, and there were vortices formed around the bubbles, while the P2 hole was still at the bottom of the molten pool and continued to undergo deformation, only at the top of the P2 hole formed a higher flow rate of fluid, and failed to form a vortex. At 180 μs, the P3 hole has moved to the top of the molten pool under the action of the vortex and is about to escape from the molten pool, and the bubbles gradually become smaller, while the P2 hole is still at the bottom of the molten pool, neither vortices are formed around the porosity, nor porosity movement occurs, and only relatively drastic deformation occurs. When the time reached 195 μs, the P3 hole had completely escaped from the molten pool and was eliminated, but the violent whirlpool flow still existed. At this time, the P2 hole was also divided into two small bubbles by the molten pool fluid under the action of the Marangoni effect, but because it was always at the bottom of the molten pool, no fluid vortex was formed, and the porosity did not move greatly. Finally, P2 formed small pores with a diameter of φ_5 μm, which were retained.

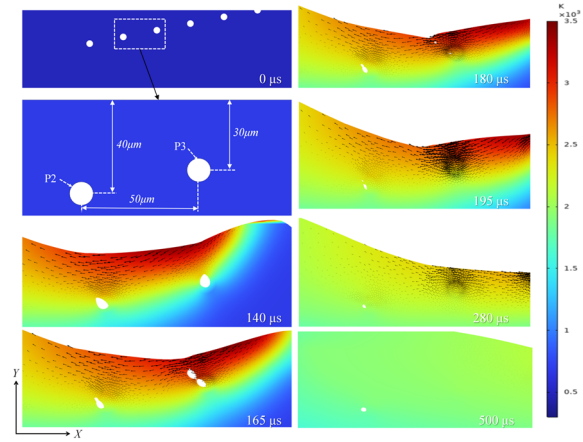

Fig. 2. The typical residual and elimination process of pores under scanning power of 100 W and scanning speed of 1 m/s

It is worth noting that at 195 μs, the pores escape and disappear completely. The maximum escape velocity is 9.73 m/s. It is worth noting that during the disappearance of pores, the pores follow the trend of backward movement of the fluid in the molten pool, rather than simply floating up in a straight line. This phenomenon can also be observed in pore evolution at other scanning speeds and laser power (as shown in Fig. 3 and Fig. 4).

To sum up, in the process of pore evolution, pores do not rise vertically but move to the tail area of the molten pool at the same time. The essence of pore evolution is mass transfer. At the microscopic scale, the evolution of pore is heavily influenced by the Marangoni effect. Fluid mass transfer caused by Marangoni effect has a significant effect on pore evolution. In the process of laser remelting, due to the rapid melting of pores and the uneven heat transfer, the pores inside the molten pool will evolve into many bubbles. Under the effect of the Marangoni effect, the fluid in the molten pool forms a vortex along the surface of the bubble, and the flow of the vortex moves from the hot area (the top of the hole) to the cold area (the bottom of the hole). This movement causes the bubble to rise, which can help the bubble escape and eliminate. When the pore depth is shallow, the Marangoni effect will cause the molten fluid at the top of the pore to move to both sides, and the pore will not be able to escape and eventually form the surface pore. On the contrary, when the pores are too deep, the molten pool fluid cannot form eddy currents around the pores to make the pores rise, so the pores cannot be eliminated eventually, resulting in the preservation of pores.

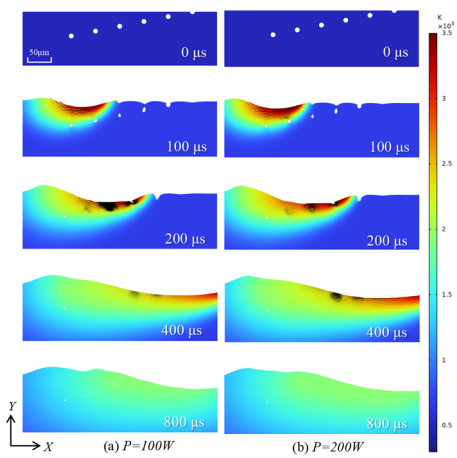

Fig. 3. Evolution of pores at a scanning speed of $V = 1$ m/s

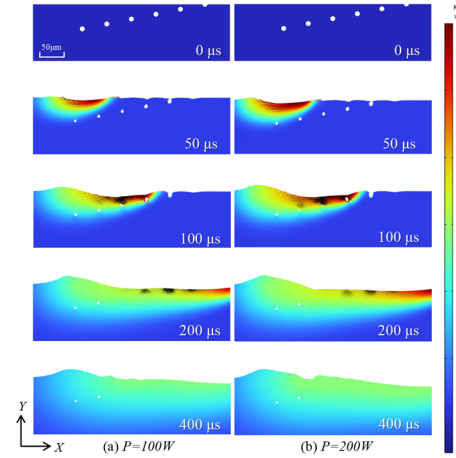

Fig. 4. Evolution of pores at a scanning speed of $V = 2$ m/s

4. Experimental results

The SLM-316L stainless steel specimens used in the experiment were fabricated via aDiMetal-100 SLM system (Guangzhou Raycus Additive Manufacturing Technology Co., Ltd.), with gas-atomized 316L stainless steel spherical powder (particle size distribution: 15-53 μm) as the feedstock. To quantitatively characterize the internal pore features of the as-fabricated specimens, micro-computed tomography (Micro-CT) was employed for three-dimensional imaging. The pore evolution before and after laser remelting is illustrated in Fig. 5: distinct keyhole defects were observed in the as-fabricated specimens, while after laser remelting, the keyhole defects were completely eliminated, leaving only a few small gas pores.

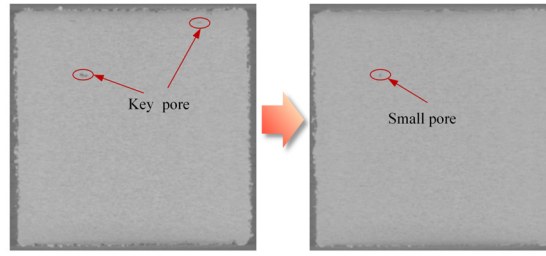

Fig. 5. Comparison of porosity between the samples before and after laser remelting

5. Conclusions

In this paper, a level set based multi-physical finite element model is established. Based on this model, the pore evolution mechanism during laser remelting is analyzed in detail. From this research, several conclusions can be drawn:

1) Based on the systematic simulation analysis of the molten pool behavior and pore evolution during the SLM forming process, the results show that the laser remelting technology can significantly reduce the internal pore defects of the formed parts by regulating the solidification rate of the molten pool and the metallurgical bonding state. It is one of the key technical means to improve the porosity of SLM formed parts and enhance the density of components at present.

2) At the microscopic scale, the evolution of pore is significantly influenced by the Marangoni effect. Under the influence of the Marangoni effect, the porosity does not rise vertically during the evolution, but moves to the tail area of the molten pool at the same time during the rise. The

ISSN PRINT 2345-0533, ISSN ONLINE 2538-8479

essence of pore evolution is mass transfer.

3) Based on the simulation and experimental results, to maximize pore elimination efficiency during laser remelting, it is recommended to adopt a moderate energy density with a laser power of 90-110 W and a scanning speed of 1.0-1.5 m/s. Within this parameter window, the Marangoni-driven fluid flow is sufficiently activated to promote pore migration and escape, while avoiding excessive melt pool instability or incomplete remelting.

Acknowledgements

The authors have not disclosed any funding.

Data availability

The datasets generated during and/or analyzed during the current study are available from the corresponding author on reasonable request.

Conflict of interest

The authors declare that they have no conflict of interest.

References

[1] E. Yasa and J.-P. Kruth, "Microstructural investigation of selective laser melting 316L stainless steel parts exposed to laser re-melting," *Procedia Engineering*, Vol. 19, pp. 389–395, Jan. 2011, https://doi.org/10.1016/j.proeng.2011.11.130

[2] C. Qiu et al., "Influence of laser processing strategy and remelting on surface structure and porosity development during selective laser melting of a metallic material," *Metallurgical and Materials Transactions A*, Vol. 50, No. 9, pp. 4423–4434, Sep. 2019, https://doi.org/10.1007/s11661-019-05348-0

[3] A. G. Demir and B. Previtali, "Investigation of remelting and preheating in SLM of 18Ni300 maraging steel as corrective and preventive measures for porosity reduction," *The International Journal of Advanced Manufacturing Technology*, Vol. 93, No. 5-8, pp. 2697–2709, Jul. 2017, https://doi.org/10.1007/s00170-017-0697-z

[4] T. Zhang et al., "Evolution of molten pool during selective laser melting of Ti-6Al-4V," *Journal of Physics D: Applied Physics*, Vol. 52, No. 5, p. 055302, Jan. 2019, https://doi.org/10.1088/1361-6463/aaee04

[5] M. Xia, D. Gu, G. Yu, D. Dai, H. Chen, and Q. Shi, "Selective laser melting 3D printing of Ni-based superalloy: understanding thermodynamic mechanisms," *Science Bulletin*, Vol. 61, No. 13, pp. 1013–1022, Jul. 2016, https://doi.org/10.1007/s11434-016-1098-7

[6] M. Courtois, M. Carin, P. L. Masson, S. Gaied, and M. Balabane, "A new approach to compute multi-reflections of laser beam in a keyhole for heat transfer and fluid flow modelling in laser welding," *Journal of Physics D: Applied Physics*, Vol. 46, No. 50, p. 505305, Dec. 2013, https://doi.org/10.1088/0022-3727/46/50/505305

[7] B. Shen et al., "Influence of laser post-processing on pore evolution of Ti-6Al-4V alloy by laser powder bed fusion," *Journal of Alloys and Compounds*, Vol. 818, p. 152845, Mar. 2020, https://doi.org/10.1016/j.jallcom.2019.152845

[8] F. Verhaeghe, T. Craeghs, J. Heulens, and L. Pandelaers, "A pragmatic model for selective laser melting with evaporation," *Acta Materialia*, Vol. 57, No. 20, pp. 6006–6012, Dec. 2009, https://doi.org/10.1016/j.actamat.2009.08.027

[9] Z. Fan and F. Liou, "Numerical modeling of the additive manufacturing (AM) processes of titanium alloy," *Titanium Alloys – Towards Achieving Enhanced Properties for Diversified Applications*, pp. 3–28, Mar. 2012, https://doi.org/10.5772/34848

[10] S. A. Khairallah, A. Anderson, A. M. Rubenchik, J. Florando, S. Wu, and H. Lowdermilk, "Simulation of the main physical processes in remote laser penetration with large laser spot size," *AIP Advances*, Vol. 5, No. 4, p. 04712, Apr. 2015, https://doi.org/10.1063/1.4918284

[11] S. I. Anisimov, "Vaporization of metal absorbing laser radiation," in *World Scientific Series in 20th Century Physics*, World Scientific, 2012, pp. 14–15, https://doi.org/10.1142/9789814317344_0002